



ELSEVIER

Contents lists available at SciVerse ScienceDirect

## Biosensors and Bioelectronics

journal homepage: [www.elsevier.com/locate/bios](http://www.elsevier.com/locate/bios)

# Poly(dopamine) coated gold nanocluster functionalized electrochemical immunosensor for brominated flame retardants using multienzyme-labeling carbon hollow nanochains as signal amplifiers

Mouhong Lin<sup>a</sup>, Yingju Liu<sup>a,\*</sup>, Xiaofen Chen<sup>a</sup>, Shidong Fei<sup>b</sup>, Chunlin Ni<sup>a</sup>, Yueping Fang<sup>a</sup>, Chengbin Liu<sup>c</sup>, Qingyun Cai<sup>c</sup>

<sup>a</sup> Institute of Biomaterials, College of Sciences, South China Agricultural University, Guangzhou 510642, China

<sup>b</sup> Shenzhen Water Quality Center, Shenzhen 518036, China

<sup>c</sup> State Key Laboratory of Chemo/Biosensing and Chemometrics, Hunan University, Changsha 410082, China.

## ARTICLE INFO

## Article history:

Received 24 September 2012

Received in revised form

8 January 2013

Accepted 23 January 2013

Available online 9 February 2013

## Keywords:

Immunosensor

Brominated flame retardants

3-Bromobiphenyl

Polydopamine

Carbon hollow nanochains

## ABSTRACT

An electrochemical, signal amplified immunosensor was developed to detect 3-bromobiphenyl (BBP) by using a bio-inspired polydopamine (PDOP)/gold nanocluster (AuNc) as the sensor platform and multienzyme-labeled carbon hollow nanochains as the signal amplifier. The self-polymerized dopamine membrane on the AuNc-modified indium tin oxide (ITO) electrode were characterized by scanning electron microscopy (SEM), atomic force microscopy (AFM), contact angle and electrochemical measurements. Such PDOP/AuNc platform featured the mild cross-linking reaction with the dense immobilization of BBP-antigens (BBP-Ag). Moreover, by using multiple horseradish peroxidase (HRP) and secondary antibodies (Ab<sub>2</sub>) modified one-dimensional carbon hollow nanochains (CHNc) as the signal enhancer, it held promise for improving the sensitivity and detection limit of the immunoassay. Based on the competitive immunoassay protocol, this immunosensor showed a linear range from 1 pM to 2 nM for BBP with a detection limit of 0.5 pM. Also, it exhibited high sensitivity, wide linear range, acceptable stability and reproducibility on a promising immobilization platform using a novel signal amplifier, which may extend its application in other environmental monitoring.

© 2013 Elsevier B.V. All rights reserved.

## 1. Introduction

In the past several decades, brominated flame retardants (BFRs) have been widely used to reduce fire risk including household electrical appliances and textiles, due to their low cost and high antflaming efficiency (Birnbbaum and Staskal, 2004). The wide distribution of BFRs and their persistent nature in the environment can not only bring the environmental safety (Kimbrough, 1987; Covaci et al., 2011), but also cause several potential risks to human health, since they can cause endocrine disruption, immunotoxicity and neurotoxicity on wildlife and humans, including liver enzyme induction, activation of the aryl hydrocarbon receptor, thyroid hormone homeostasis disruption and vitamin A level disruption (Munschy et al., 2011; Tanabe, 2008; Brown et al., 2004). Therefore, the sensitive detection of BFRs has become a significant subject. Electrochemical biosensing has been regarded as a promising technique to monitor BFRs (Centi et al., 2007; Laschi et al., 2003), owing to its high sensitivity, rapid response and low cost (Kimmel

et al., 2012). To achieve a much higher selectivity and sensitivity, the electrochemical immunosensing has recently attracted considerable interest since different immobilization methods and labeling technologies were explored for the signal amplification (Ricci et al., 2007).

Firstly, the stability and activity of the immobilized biocomponent was crucial for the sensitivity of immunosensors. Various functional polymers have brought remarkable innovation in the construction of biosensors (Haddour et al., 2006; Lin et al., 2012b). Especially, by combining those stable and versatile polymers with nanogold, novel biosensors were fabricated, such as nanogold deposited poly(terthiophene) immunosensor for osteoproteogelin (Singh et al., 2008), polypyrrole–nanogold functionalized immunosensor for hemoglobin (Qu et al., 2009), polyaniline–gold hybrid nanocomposite based immunosensor for prostate specific antigen (Dey et al., 2012) and nanogold/poly(dopamine) based immunosensor for Interleukin-6 (Wang et al., 2011a). By a simple dip-coating process, the mussel-inspired polydopamine (PDOP) film, possessing versatile function such as substrate adhesion, electrodeless metallization and facile conjugation (Lee et al., 2007a, 2007b, 2009), exhibited attractive application in chemical, electronic and biochemical fields (Lee et al., 2007a, 2006). Importantly, the strong

\* Corresponding author. Tel.: +86 20 85280325; fax: +86 20 85282366.  
E-mail address: liuyingju@hotmail.com (Y. Liu).

substrate adhesion of PDOP allowed its formation and attachment on various surfaces including metals, oxides, semiconductors, ceramics and synthetic polymers (Lee et al., 2007a). Moreover, as a product from the self-oxidative polymerization of dopamine (2-(3,4-dihydroxyphenyl) ethylamine), it comprised an aromatic structure with catechol group, which was able to capture biomolecule based on nucleophilic reaction or Schiff base reaction between the catechol group of PDOP and the amino group of protein (Lee et al., 2009), such as portable PDOP modified optical immunosensor for Human IgG (Liu et al., 2012), PDOP/CNT modified cytosensor for myoblast cells (Zheng et al., 2012), PDOP modified immunosensor for sulfate-reducing bacteria (Wan et al., 2011b) and PDOP-like polymer based substrate for DNA immobilization (Ham et al., 2011). In this work, such PDOP film was assembled on 3-D gold nanocluster (AuNc) to capture antigen. Compared with colloidal gold immobilization (Dey et al., 2012; Qu et al., 2009; Wang et al., 2011a), the covalent bond by PDOP immobilization was stronger than the adsorption of colloidal gold, and the mild reaction between PDOP and antigen can preserve protein activity (Lee et al., 2009).

Moreover, signal amplification based on bio-nanomaterial can not only produce a synergic effect among catalytic activity, conductivity and biocompatibility, but also provide amplified signals by high loading of signal tags (Lei and Ju, 2012). Carbon nanomaterial has been extensively employed as multi-labeling amplification (Yang et al., 2010), including carbon nanotube (Wang et al., 2011a; Zhu et al., 2010), graphene (Du et al., 2011; Wan et al., 2011a) and carbon sphere (Du et al., 2010; Lin et al., 2012a). Recently, our team proposed a new type of nanoarchitecture, SnO<sub>2</sub>@carbon core-shell nanochains (SCNCs), which achieved satisfactory performance in lithium-ion batteries (Yu et al., 2011; Zhang et al., 2010) and direct methanol fuel cells (Yang et al., 2012). Interestingly, a well-defined novel nanostructure of carbon hollow nanochain (CHNc) was found when SCNCs were processed under 800 °C at a high argon flow rate. Such 1-D hollow nanostructure of CHNc was expected to provide fast electron transfer and dense immobilization of protein owing to its high surface-to-volume ratio and surface activity (Zhang et al., 2010). Then, multi-HRP-CHNc-Ab<sub>2</sub> was prepared as the electrochemical signal amplifier by loading a large amount of horseradish peroxidase (HRP) and HRP-labeled secondary antibody (HRP-Ab<sub>2</sub>) on CHNc.

In this work, a new antibody of 3-bromobiphenyl (BBP) was produced by immunizing New Zealand white rabbit with BBP-antigen (BBP-Ag), and then an electrochemical immunosensor was fabricated for sensitive detection of BFRs based on a dual amplification mechanism from the PDOP coated Au nanocluster (PDOP/AuNc) sensor platform and the multi-HRP-CHNc-Ab<sub>2</sub> signal amplifier. Basing on the competitive immunoassay, BBP-Ag on the electrode competed with the free analyte in the solution to capture anti-BBP antibody (BBP-Ab<sub>1</sub>). The electrochemical signal of the captured multi-HRP-CHNc-Ab<sub>2</sub> label was efficiently recorded by the catalytic reaction of HRP with the hydrogen peroxide (H<sub>2</sub>O<sub>2</sub>)-hydroquinone (HQ) system.

## 2. Experimental

### 2.1. Materials and instruments

Gold (III) chloride tetrahydrate and 2-amino-2-hydroxymethylpropane-1,3-diol (Tris, C<sub>4</sub>H<sub>11</sub>NO<sub>3</sub>) were purchased from Shanghai Chemical Reagent Co., Ltd. N-(3-Dimethylaminopropyl)-N'-ethylcarbodiimide hydrochloride (EDC), N-hydroxysuccinimide (NHS), 3-bromobiphenyl (BBP) and hydroxybiphenyl (C<sub>12</sub>H<sub>10</sub>O) were bought from J&K Chemical Company. Dopamine hydrochloride

(C<sub>8</sub>H<sub>11</sub>NO<sub>2</sub>·HCl) was from Aladdin Chemistry Co., Ltd. HRP, ovalbumin (OVA) and bovine serum albumin (BSA) were purchased from Roche Company. HRP-labeled secondary chicken anti-rabbit antibody (HRP-Ab<sub>2</sub>, 400 μg mL<sup>-1</sup>) were bought from Santa Cruz.

Phosphate-buffered saline with 0.05% (v/v) Tween 20 (PBST, 0.01 M, pH 7.4) was prepared by dissolving 2.9 g Na<sub>2</sub>HPO<sub>4</sub>·12H<sub>2</sub>O, 0.2 g KH<sub>2</sub>PO<sub>4</sub>, 8.5 g NaCl, 0.2 g KCl and 0.5 mL Tween 20 into 1 L water, which was used as the diluent for the immunoreagent and washing buffer in the experiment. BBP stock solution (10<sup>-2</sup> M) was prepared by dissolving BBP into ethanol and diluted to various concentrations by PBS 7.4 containing 4% ethanol.

The surface of PDOP/AuNc was observed by scanning electron microscopy (SEM, JEOL JIB-4600F, Japan) and atomic force microscope (AFM, Being CSPM 5500, China). AFM measurement was operated in tapping mode and analyzed by the CSPM Imager software. Transmission electron microscope (TEM) (Tecnai 12, FEI, Holland) and FTIR Spectrometer (Nicolet Avatar 360, Thermo, America) were used to characterize the morphology and surface groups of CHNc, respectively. All electrochemical experiments were performed on a CHI660D electrochemical workstation (Chenhua Instruments Co. Ltd., Shanghai, China) with a three-electrode system composing a modified indium tin oxide (ITO) electrode (0.35 cm<sup>2</sup>) as working electrode, a saturated Ag/AgCl electrode as reference electrode and a platinum sheet electrode as counter electrode.

### 2.2. Preparation of antigen and antibody

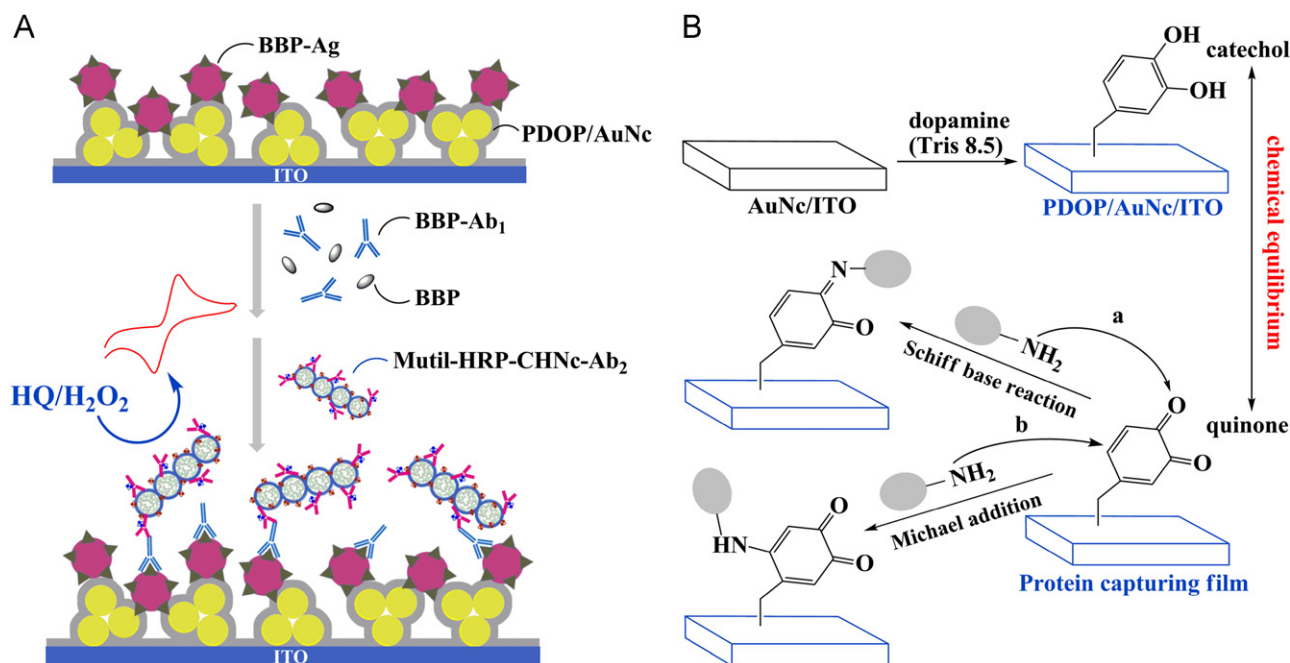
Firstly, 3-bromo-4-hydroxybiphenyl (C<sub>12</sub>H<sub>9</sub>OBr) was synthesized by the reaction of *p*-hydroxybiphenyl (C<sub>12</sub>H<sub>10</sub>O) and Br<sub>2</sub> in glacial acetic acid with ferrous powder as the catalyst. The product was purified by column chromatography on silica gel using petroleum ether/ethyl acetate (25/1) as the eluent. Then, the hapten of BBP, 3-bromo-4-hexanoic acid-biphenyl (C<sub>18</sub>H<sub>19</sub>O<sub>3</sub>Br) was prepared by 6-bromocaproic acid with C<sub>12</sub>H<sub>9</sub>OBr. <sup>1</sup>HNMR (400 MHz, CDCl<sub>3</sub>): δ11.2 (1H, s), δ7.78 (1H, s), δ7.55 (2H, d, J=8.4 Hz), δ7.46 (1H, d, J=8.4 Hz), δ7.42 (2H, t, J=7.6 Hz), δ7.32 (1H, t, J=7.4 Hz), δ6.94 (1H, d, J=8.4 Hz), δ4.07 (2H, t, J=6.2 Hz), δ2.44 (2H, t, J=7.4 Hz), δ1.93 (2H, q, J=7.0 Hz), δ1.78 (2H, q, J=7.0 Hz), δ1.65 (2H, q, J=7.0 Hz). MS *m/z*=363 [M]<sup>+</sup>, calculated for C<sub>18</sub>H<sub>19</sub>O<sub>3</sub>Br=363.25.

Hapten was coupled to BSA/OVA as immunogen/antigen by the active ester method. Briefly, 0.05 mmol hapten and 0.15 mmol EDC were dissolved in 200 μL DMF. Then, 0.15 mmol NHS was added and the solution was stirred for 5 h. After the white precipitate was removed by centrifugation, the supernatant was added dropwise to BSA or OVA in 3 mL carbonate buffer (pH 9.6), keeping the ratio of hapten with protein at 100:1. The mixture was stirred at 4 °C for 12 h, and then dialyzed with 10 mM PBS (pH 7.4) for 3 days.

Two New Zealand white male rabbits weighing between 2.5 and 3 kg were used at the Guangdong Medical Laboratory Animal Center. The rabbits were immunized with hapten-BSA in Freund's complete adjuvant under aseptic conditions for the first time. Then, the immunization was repeated 4 times in 3 week intervals. One week after the third immunization, blood samples were collected from ear vein of the rabbit and the titer was examined by ELISA using 3,3',5,5'-tetramethylbenzidine and H<sub>2</sub>O<sub>2</sub> as the substrate (Lei et al., 2010; Wang et al., 2011b). Finally, 1 week after the last immunization, the rabbits were killed and the blood was collected, which was kept at 4 °C overnight and centrifuged at 5000 r/min for 10 min. The serum was stored in glycerol (v:v=1:1) at -20 °C when not in use.

### 2.3. Preparation of CHNc

The CHNc was prepared according to our previous work with a little modification (Zhang et al., 2010). Typically, 0.324 g



**Scheme 1.** (A) PDOP/AuNc platform for competitive immunoassay of BBP with the multi-HRP-CHNc-Ab<sub>2</sub> conjugate as signal amplifier. (B) PDOP coating and one-step protein immobilization through the reaction between amino groups of proteins and PDOP-coated substrates.

Na<sub>2</sub>SnO<sub>3</sub> · 3H<sub>2</sub>O and 6 g D-glucose were dissolved in 40 mL water, and transferred into a 50 mL Teflon-lined stainless steel autoclave. Then, the precipitate was heated at 180 °C for 4 h, followed by washing with water and ethanol twice, respectively. After it was dried at 50 °C overnight, the product was heated to 800 °C at a rate of 5 °C min<sup>-1</sup>, held at 800 °C for 4 h and cooled down in Ar atmosphere. Finally, it was treated by sonication in 2 M H<sub>2</sub>SO<sub>4</sub>, stirred overnight, washed and dried at 50 °C, CHNc was then obtained.

#### 2.4. Preparation of multi-HRP-CHNc-Ab<sub>2</sub> conjugate

Typically, 1.0 mg of CHNc was dispersed into 2.0 mL of water. After sonication for 30 min, the dispersion was mixed with 10 mg EDC and 1.4 mg NHS, followed by washing with water twice. The precipitate was then redispersed into 1 mL PBST (pH 7.4) and ultrasonicated for 10 min. Then, it was gently mixed with 4 mg mL<sup>-1</sup> HRP and 20 μg mL<sup>-1</sup> HRP-Ab<sub>2</sub>, and stirred at 4 °C overnight. After centrifugation at 12,000 rpm for 15 min, the product was washed with PBST twice. Finally, it was dispersed in 1 mL PBST and stored at 4 °C when not in use.

#### 2.5. Fabrication of the immunosensor

As shown in Scheme 1A, the PDOP–AuNc platform worked as the sensor surface. A cleaned ITO electrode was scanned in 0.5 mM HAuCl<sub>4</sub> (in 0.5 M H<sub>2</sub>SO<sub>4</sub>) in the range from –0.3 to 0.3 V for 5 cycles at a scan rate of 50 mV s<sup>-1</sup>. According to earlier work (Lee et al., 2009), PDOP was coated onto AuNc/ITO by dropping 40 μL of 2 mg mL<sup>-1</sup> of dopamine in 10 mM Tris buffer (pH 8.5) onto the electrode surface and sealing for 12 h, followed by rinsing and drying.

For the antigen immobilization, 40 μL of BBP-Ag solution (1:50, 30.04 μg mL<sup>-1</sup>) was spread onto the PDOP/AuNc surface. The electrode was incubated at 4 °C overnight and rinsed with PBST. Then, it was incubated in 30 μL of 5% skim milk at 37 °C for 1 h to prevent the nonspecific binding.

For the competitive immunoreaction, 5 μL of BBP sample was rapidly mixed with 45 μL of BBP-Ab<sub>1</sub> (1:60, 9.57 μg mL<sup>-1</sup>), and then a portion (30 μL) of the mixture was dropped onto the Ag/PDOP/AuNc surface. The competitive reaction was conducted at 37 °C for an hour. After washing, the electrode was incubated with 30 μL of multi-HRP-CHNc-Ab<sub>2</sub> solution for another 60 min. The electrochemical signal was collected in 1/15 M PBS containing 1 mM HQ, which was characterized by cyclic voltammetry between –0.6 V and 0.8 V before and after the addition of 1.5 mM H<sub>2</sub>O<sub>2</sub>.

### 3. Results and discussions

#### 3.1. Characterization of the PDOP/AuNc platform

As shown in Scheme 1B, the PDOP/AuNc platform was used to immobilize the antigen. The catechol groups of the PDOP film can chemically capture the amino groups of BBP-Ag based on nucleophilic reactions or Schiff base reactions (Lee et al., 2009). The digital images of ITO electrode surfaces were shown in the supporting information (Supporting information: Fig. S1). Compared with bare ITO (Fig. S1a), a light blue layer (Fig. S1b) can be observed after the electrodeposition, which further changed to dark blue after PDOP was formed (Fig. S1c).

Fig. 1A and B was SEM images of AuNc before and after PDOP modification. As shown in Fig. 1A, it revealed that a relatively monodispersed AuNc with average cluster diameter of about 60 nm was successfully assembled on the electrode surface. Fig. 1B was SEM image of PDOP/AuNc on ITO, where a different nanostructure can be observed, indicating PDOP film has been formed on AuNc.

AFM analysis can provide useful information on the surface property of the sensor. Bare ITO (Fig. 1C) was relatively smooth with an average surface roughness of 2.05 ± 0.12 nm and a surface area of 170.4 μm<sup>2</sup>, which was calculated by the CSPM Imager software. After the assembly of AuNc/PDOP, a densely packed nanostructure layer was observed (Fig. 1D), suggesting that AuNc/PDOP achieved

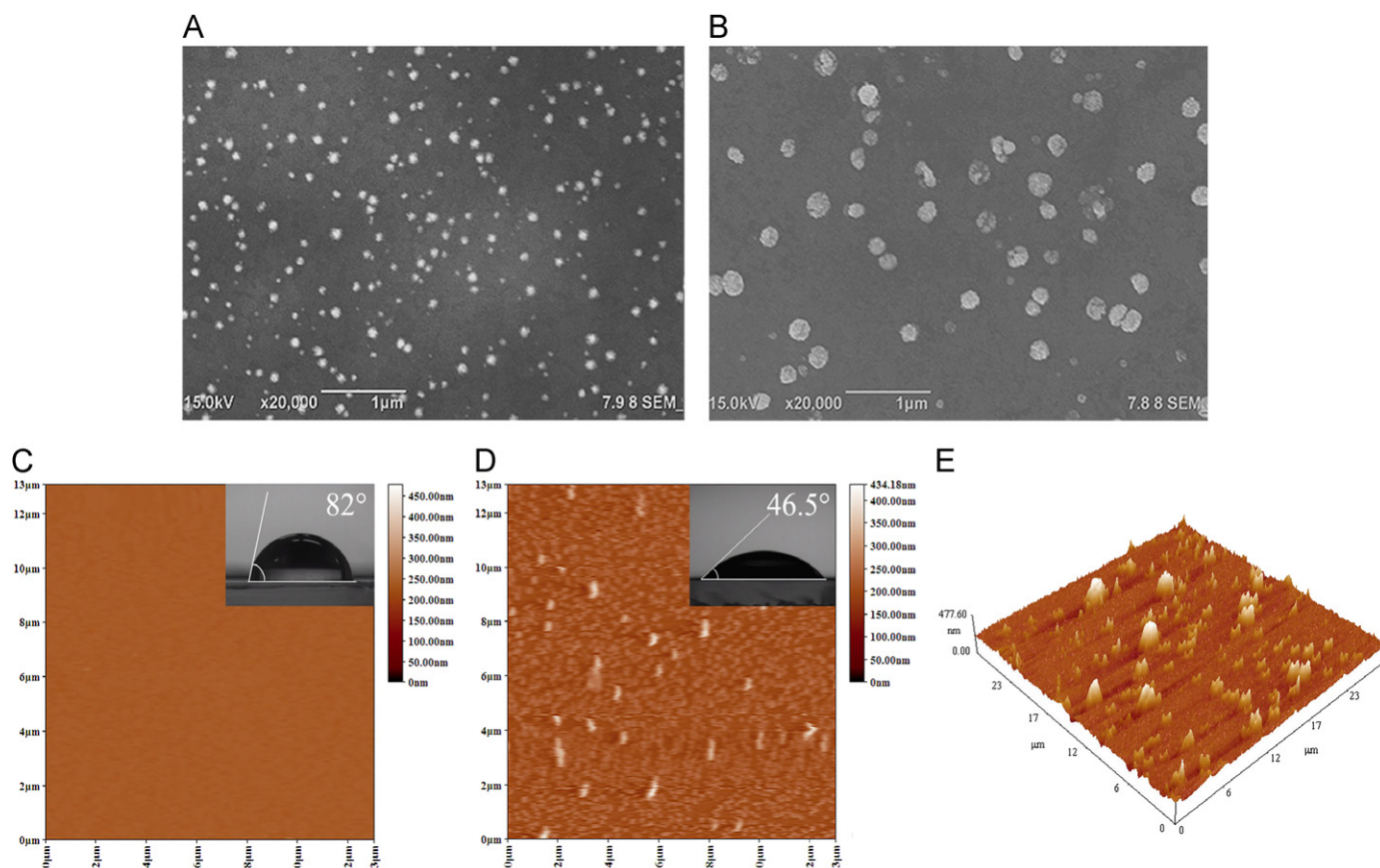


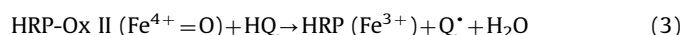
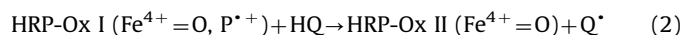
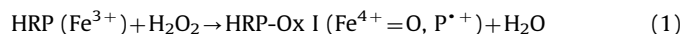
**Fig. 1.** SEM images of (A) the electrodeposited AuNc and (B) PDOP coated AuNc on ITO. Tapping mode AFM of (C) bare ITO, (D) PDOP/AuNc/ITO and (E) 3D image of BBP-Ag/PDOP/AuNc/ITO.

nearly complete coverage on ITO. The average surface roughness was  $14.7 \pm 2.0$  nm, with an 11-fold increase in surface area over bare ITO, indicating the successful increase in PDOP active sites. Fig. 1E displays the three-dimensional AFM image after the immobilization of BBP-Ag. A rolling hill-like appearance was observed, which was generally characteristic of globular protein coated on a rough surface (Balamurugan and Chen, 2008; Mani et al., 2009). Furthermore, the biocompatibility of the sensor surface can be characterized by its hydrophilicity from the contact angle measurement, which can be found in the inset of the corresponding AFM image. Comparing with bare ITO, the contact angle did not change significantly (from  $82^\circ$  to  $80.5^\circ$ ) after AuNc coating (Supporting information: Fig. S1), while that of PDOP/AuNc/ITO dramatically decreased to  $46.5^\circ$ , indicating the PDOP-modified ITO could provide a more hydrophilic surface for protein immobilization.

In addition, the electrochemical characterization of the PDOP/AuNc platform was discussed in detail (Supporting information: Fig. S2). In Fig. S2A, cyclic voltammogram for bare ITO (line a) showed a relatively low current response due to the relatively low activity of ITO surface. When a thin layer of PDOP was directly formed on ITO (Fig. S2A, line b), the current increased a little, suggesting the electron transfer was improved by the electrochemical activity of PDOP. However, if AuNc was decorated on ITO surface before PDOP film, the AuNc/PDOP (Fig. S2A, line c) exhibited a much larger current increase from  $-0.6$  to  $-0.2$  V, indicating a further increase in the conductivity of the platform.

The protein capturing property of the platform was studied by direct immobilization of HRP onto the PDOP/AuNc surface. Briefly,  $30 \mu\text{L}$  of  $4 \text{ mg mL}^{-1}$  HRP was spread on the PDOP/AuNc electrode and incubated overnight. Electrochemical measurements were performed in  $10 \text{ mL}$  PBS buffer (pH 7.4) containing  $1 \text{ mM}$  HQ. Fig. S2B

displays the cyclic voltammograms without (d) and with (e) the addition of  $0.5 \text{ mM}$   $\text{H}_2\text{O}_2$ . Compared with curve d, a decrease in oxidation peak and an increase in reduction peak can be found after the addition of  $\text{H}_2\text{O}_2$  (curve e), which was characteristic of the enzyme-catalyzed electrochemical reduction. During the process, HRP reduced  $\text{H}_2\text{O}_2$  to  $\text{H}_2\text{O}$  by a 2-electron pathway through its oxidative state (HRP-Ox), which can be described as follows:



In the above reactions, HRP ( $\text{Fe}^{3+}$ ) stands for the native enzyme and HRP-Ox I refers to an oxidized form of HRP consisting of an oxyferryl Fe ( $\text{Fe}^{4+}=\text{O}$ ) and porphyrin  $\pi$  cation radical ( $\text{P}^{\bullet+}$ ) (Ferapontova et al., 2001). HRP-Ox I is then reduced to native HRP by an electron donor (HQ) in two steps, where HQ stands for hydroquinone. The formed oxidized donor,  $\text{Q}^{\bullet}$ , is then electrochemically reduced by the electrode. Therefore, the observed current is relative to  $\text{Q}^{\bullet}$  concentration in the solution, which depends on the content of HRP. The change of reduced current ( $\Delta I$ ) before and after the addition of  $\text{H}_2\text{O}_2$  was adopted as the detection signal.

### 3.2. Characterization of CHNc and multi-HRP-CHNc- $\text{Ab}_2$ conjugates

Briefly,  $\text{SnO}_2@\text{CPS}$  was synthesized by the hydrothermal method (Zhang et al., 2010). Such precursor was subsequently treated under  $800^\circ\text{C}$  at a high argon flow rate, when a visible

layer with metal luster can be found around the crucible after calcination. It can be regarded as a result of the carbothermic reduction reaction between  $\text{SnO}_2$  and the carbon shell, since Sn was easy to melt (m.p.: 232 °C; Zou and Wang, 2011) and then escaped from the shell. In Fig. 2A, TEM demonstrated a distinct hollow ring-like superstructure resulting from the exsolution of core material, which was very different from earlier works (Zhang et al., 2010; Yu et al., 2011). Moreover, in the XRD pattern (Fig. 2B), the peaks of  $\text{SnO}_2$  disappeared (Yu et al., 2011) and a characteristic XRD pattern of Sn was observed (JCPDS file, 86-2265), further indicating that  $\text{SnO}_2$  nanoclusters were fully dissolved.

The surface functional groups of CHNc were critical for the subsequent fabrication of the multi-HRP-CHNc- $\text{Ab}_2$  conjugate. In Fig. 2C, the strong characteristic peak at  $3428\text{ cm}^{-1}$  was related to the stretching vibration of hydroxyl group, while the absorption peaks at  $1590\text{ cm}^{-1}$  and  $1250\text{ cm}^{-1}$  were attributed to the asymmetric and symmetric stretching vibrations of  $\text{COO}^-$  group, respectively, suggesting the existence of available carboxyl group on CHNc surface (Lin et al., 2012a; Sun and Li, 2004), which can be activated by EDC/NHS to form an intermediate ester with the amine residues of protein (Lin et al., 2011; Yu et al., 2006). Fig. 2D shows the UV-vis absorption of the as-prepared conjugate (a), CHNc (b), HRP (c) and  $\text{Ab}_2$  (d). The CHNc carriers (curve b) showed no distinct UV-vis absorption in PBS buffer. However, a strong absorption peak located at 410 nm and a relatively weak peak appeared at about 280 nm were found from the multi-HRP-CHNc- $\text{Ab}_2$  conjugate (curve a). The peak dominated at 280 nm, similar to curve d, was typical absorption of protein, whose intensity was relative with the protein content. However, comparing with HRP (curve c), the ratio of peak intensity at 280 nm and 410 nm increased for the conjugate (curve a), indicating the peak dominated at 280 nm for the conjugate may be an overlay of  $\text{Ab}_2$  and HRP.

### 3.3. Optimization of detection conditions

The influence of dilution ratios of BBP-Ag, BBP- $\text{Ab}_1$  and multi-HRP-CHNc- $\text{Ab}_2$  conjugate were studied in detail (Supporting information: Fig. S3). Fig. S3A displays the relationship between the BBP-Ag concentration and the signal intensity. A linear increase of  $\Delta I$  was found from 400-fold dilution to 100-fold dilution, and tended to level off after 100-fold dilution. Thus, the 100-fold dilution was selected as the optimal antigen dilution ratio. Moreover, the amount

of  $\text{Ab}_1$  was critical in the competitive immunoassay. Excessive  $\text{Ab}_1$  will result in inefficient competition, while insufficient  $\text{Ab}_1$  will lead to a narrow detection range. Fig. S3B shows the optimization curve of  $\text{Ab}_1$  concentration ranging from 160-fold dilution to 40-fold dilution.  $\Delta I$  increased sharply with the increase of  $\text{Ab}_1$  concentration, peaking at 60-fold and then started to decrease, indicating that the 60-fold dilution was the optimal concentration. Furthermore, the dilution ratio of multi-HRP-CHNc- $\text{Ab}_2$  conjugate was optimized as 2-fold (Fig. S3C). Finally, the effect of pH of the working buffer was studied between 5.29 and 8.67 in PBS. As shown in Fig. S3D, the amperometric response increased from 5.29 to 6.81 and decreased from pH 6.81 to 8.67. Therefore, PBS of pH 6.81 was selected.

### 3.4. The enhancement of the electrochemical signal by the signal amplified immunosensor

Fig. 3A showed the detection performance of the immunosensor using conventional HRP- $\text{Ab}_2$  as the detection label. The current response of the PDOP modified immunosensor (Fig. 3A, inset a) with 0.2 nM BBP was  $30.9\text{ }\mu\text{A}$ , while the response of the PDOP/AuNc modified immunosensor was  $49.1\text{ }\mu\text{A}$  (Fig. 3A, inset b), indicating such PDOP/AuNc structure immobilized much more antigens. In addition, the response of the PDOP/AuNc modified immunosensor decreased with the increase in BBP concentration, indicating BBP can efficiently inhibit the antigen-antibody reaction. A linear relationship between  $\Delta I$  and the logarithm of the BBP concentration was found as  $\Delta I = 40.6 - 10.6\lg[\text{BBP}]$  in the range of 0.02 and 2 nM with a correlation coefficient of 99.5%. The sensitivity, the slope of the calibration curve, was about  $10.6\text{ }\mu\text{A}(\lg\text{nM})^{-1}$ .

As shown in Scheme 1A, the multi-HRP-CHNc- $\text{Ab}_2$  conjugate, instead of conventional HRP- $\text{Ab}_2$ , was used as the label in the electrochemical immunoassay for BBP. The current response of the PDOP/AuNc modified immunosensor for 0.2 nM BBP by using the multi-HRP-CHNc- $\text{Ab}_2$  conjugate (Fig. 3B, inset b) was  $63.2\text{ }\mu\text{A}$ , which was 28.7% larger than that of the immunosensor using the conventional HRP- $\text{Ab}_2$  label (Fig. 3A, inset b). Under the optimized conditions, Fig. 3B showed the current response of the immunosensor decreased with the increase in BBP concentrations. A linear relationship between the current response and the logarithm of BBP concentrations (Fig. 3B, inset a) was described as  $\Delta I = 91.7 - 12.2\lg[\text{BBP}]$  ( $r = 99.7\%$ ) in the range from 1 pM to 2 nM with a detection limit of 0.5 pM ( $S/N = 3$ ). The sensitivity,  $12.2\text{ }\mu\text{A}(\lg\text{pM})^{-1}$ ,

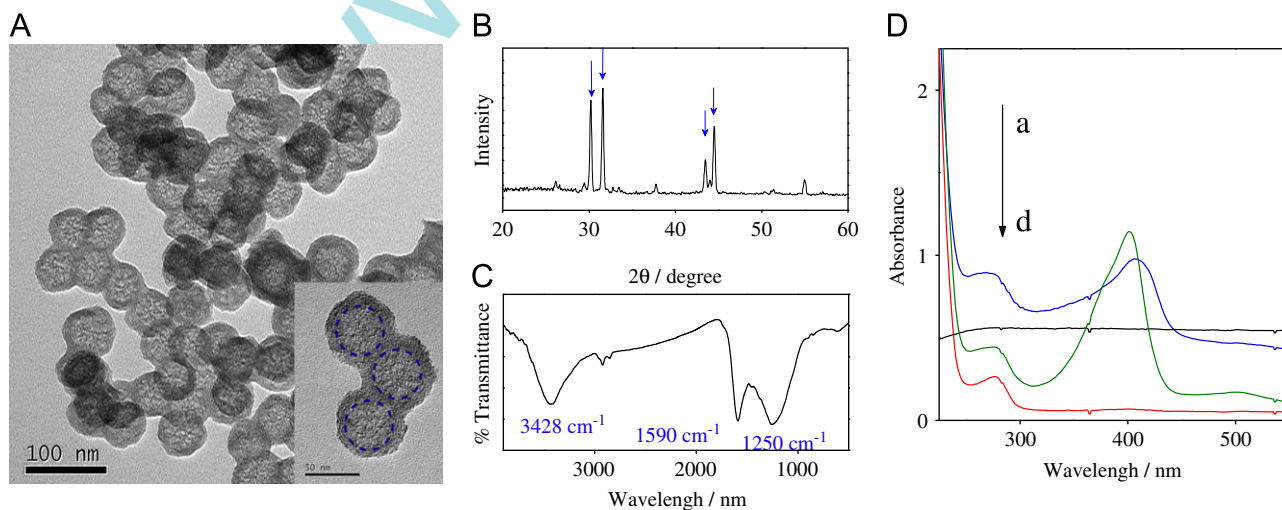
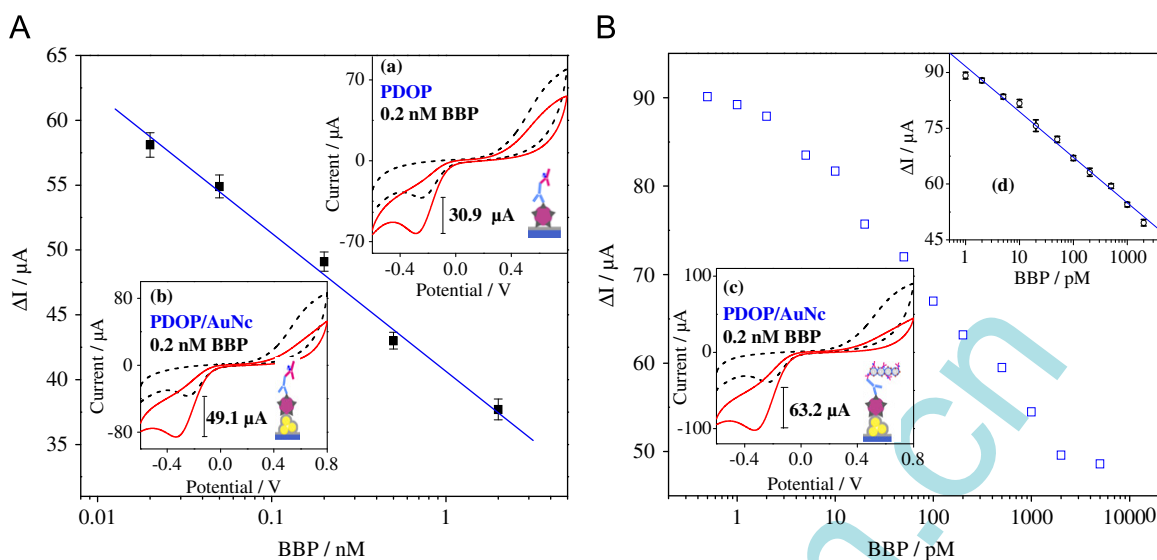
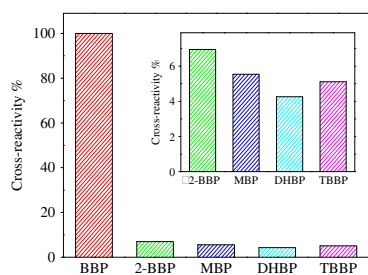


Fig. 2. TEM (A), XRD (B) and FT-IR spectra (C) of CHNc; (D) UV-vis spectra in PBS 7.4 of the as-prepared multi-HRP-CHNc- $\text{Ab}_2$  conjugate (a), CHNc (b), HRP (c) and HRP- $\text{Ab}_2$  (d).



**Fig. 3.** (A) Relationship between BBP concentrations and signal response from the PDOP/AuNc modified immunosensor using HRP-Ab<sub>2</sub> as the label. The inset was cyclic voltammogram for 0.2 nM BBP in PBS 7.4 containing 1 mM HQ without (dotted line) and with (solid line) 1.5 mM H<sub>2</sub>O<sub>2</sub> by using PDOP (a) and PDOP/AuNc (b) as the substrate, respectively. (B) Relationship between BBP concentrations and signal response from the PDOP/AuNc modified immunosensor using multi-HRP-CHNc-Ab<sub>2</sub> conjugate as the label. The inset was (c) cyclic voltammogram of such immunosensor for 0.2 nM BBP in PBS 7.4 containing 1 mM HQ without (dotted line) and with (solid line) 1.5 mM H<sub>2</sub>O<sub>2</sub>, and (d) the calibration curve of the proposed immunosensor for BBP ( $n=3$ ), respectively. Scan rate: 100 mV s<sup>-1</sup>.



**Fig. 4.** The cross-reactivity of the proposed immunosensor.

was larger than that with conventional HRP-Ab<sub>2</sub>, which was due to the increased HRP molecules by CHNc labeling.

### 3.5. Specificity, precision, reproducibility and stability of immunosensor

Specificity is a commonly evaluated parameter for the validation of antigen–antibody binding, which was determined by measuring the cross-reactivity (CR) to some structurally related compounds (Lei et al., 2010). The value of CR was calculated according to the following equation:

$$CR = \frac{C[\text{Interference}]}{C[\text{BBP}]} \times 100\% \quad (5)$$

where  $C$  stood for the apparent concentration of the analyte, including BBP, 2-bromobiphenyl (2-BBP), 4-methylbiphenyl (MBP), 4,4'-dihydroxybiphenyl (DHBP) and 2,3',5-tribromobiphenyl (TBBP). Sample of 0.2 nM BBP and interferences were exposed to the immunosensor, respectively, when the apparent concentration was calculated from  $\Delta I$  using the standard curve of BBP. As shown in Fig. 4, the CR value for 2-BBP, MBP, DHBP and TBBP were 6.95%, 5.54%, 4.26% and 5.11%, respectively, which meant the presence of those compounds cannot interfere significantly in the detection of BBP, therefore, the selectivity of the proposed immunosensor was reasonable.

The precision and reproducibility of the immunosensor was estimated by intra- and inter-assay study. The intra-assay

precision was evaluated by analyzing two concentration levels for five times by the same immunosensor, where the coefficient of variations were 6.8% and 6.2% at 10 pM and 200 pM of BBP, respectively. The inter-assay precision was evaluated by analyzing one concentration using five immunosensors, where the coefficient of variations of inter-assay were 9.5%, 8.6% and 8.5% at 20 pM, 50 pM, and 100 pM of BBP, respectively. Thus, the reproducibility of the proposed immunoassay was acceptable.

The stability of the multi-HRP-CHNc-Ab<sub>2</sub> conjugate was examined. The bioconjugate was stored in PBS 7.4 at 4 °C when not in use. The response of the bioconjugate retained about 87.5% of initial intensity after a storage period of 30 days. The stability of the fabricated immunoassay was also tested, showing that about 82.5% of initial current response was retained after 2 weeks' storage at 4 °C, indicating that the immunosensor was of acceptable stability.

### 3.6. Application in river water samples

Coastal and estuarine areas are major nursery zones for a variety of fish species, whereas they also receive contaminant inputs from various human activities. The river water from the estuary of the Pearl River was collected, and used as sample solvent. The immunosensor was evaluated by the addition of 10, 20, 50, 100 and 200 pM BBP in water sample by standard addition, in which the recoveries ranged from 96.5% to 103.8% (Supporting information: Table S1), indicating that the suitability of the immunosensor as a reliable detection method of BBP in the environmental sample.

## 4. Conclusion

In this work, a highly sensitive and selective immunosensor was successfully designed for the detection of BBP basing on a dual amplification strategy. The PDOP/AuNc substrate provided a desirable platform for the antigen immobilization through facile chemical reaction, where AuNc can improve the specific surface area and the conductivity of PDOP film. Moreover, novel one-dimensional CHNc was employed as enzyme-loading carrier for

the fabrication of multi-HRP-CHNC-Ab<sub>2</sub> conjugate, allowing higher signal response than conventional HRP-Ab<sub>2</sub>. Under the optimized conditions, the detection limit for BBP was as low as 0.5 pM with a relatively wide linear range from 1 pM to 2 nM, while the reproducibility, stability and precision were fine. Such facile protein conjugating PDOP/AuNc platform, together with the signal amplification strategy, should result in sensors and nanostructures with important applications in environmental monitoring, disease diagnosing, process control and field application.

### Acknowledgments

The work was financially supported by the Natural Science Foundation of China (21105030), the National Basic Research Program of China (2009CB421601), Shenzhen Water Development Special Fund (2012-3-84) and the Key Academic Program of 211 Project of South China Agricultural University (2009B010100001).

### Appendix A. Supporting information

Supplementary data associated with this article can be found in the online version at <http://dx.doi.org/10.1016/j.bios.2013.01.058>.

### References

- Balamurugan, A., Chen, S.M., 2008. *Biosensors and Bioelectronics* 24 (4), 976–980.
- Birnbaum, L.S., Staskal, D.F., 2004. *Environmental Health Perspectives* 112 (1), 9–17.
- Brown, D.J., Van Overmeire, I., Goeyens, L., Denison, M.S., De Vito, M.J., Clark, G.C., 2004. *Chemosphere* 55 (11), 1509–1518.
- Centi, S., Silva, E., Laschi, S., Palchetti, I., Mascini, M., 2007. *Analytica Chimica Acta* 594 (1), 9–16.
- Covaci, A., Harrad, S., Abdallah, M.A., Ali, N., Law, R.J., Herzke, D., de Wit, C.A., 2011. *Environment International* 37 (2), 532–556.
- Dey, A., Kaushik, A., Arya, S.K., Bhansali, S., 2012. *Journal of Materials Chemistry* 22 (29), 14763–14772.
- Du, D., Wang, L.M., Shao, Y.Y., Wang, J., Engelhard, M.H., Lin, Y.H., 2011. *Analytical Chemistry* 83 (3), 746–752.
- Du, D., Zou, Z.X., Shin, Y., Wang, J., Wu, H., Engelhard, M.H., Liu, J., Aksay, I.A., Lin, Y.H., 2010. *Analytical Chemistry* 82 (7), 2989–2995.
- Ferapontova, E.E., Grigorenko, V.G., Egorov, A.M., Borchers, T., Ruzgas, T., Gorton, L., 2001. *Biosensors and Bioelectronics* 16 (3), 147–157.
- Haddour, N., Chauvin, J., Gondran, C., Cosnier, S., 2006. *Journal of American Chemical Society* 128 (30), 9693–9698.
- Ham, H.O., Liu, Z.Q., Lau, K.H.A., Lee, H., Messersmith, P.B., 2011. *Angewandte Chemie International Edition* 50 (3), 732–736.
- Kimbrough, R.D., 1987. *Annual Review of Pharmacology and Toxicology* 27, 87–111.
- Kimmel, D.W., LeBlanc, G., Meschievitz, M.E., Cliffler, D.E., 2012. *Analytical Chemistry* 84 (2), 685–707.
- Laschi, S., Mascini, M., Scortichini, G., Fránek, M., Mascini, M., 2003. *Journal of Agricultural and Food Chemistry* 51 (7), 1816–1822.
- Lee, H., Dellatore, S.M., Miller, W.M., Messersmith, P.B., 2007a. *Science* 318 (5849), 426–430.
- Lee, H., Lee, B.P., Messersmith, P.B., 2007b. *Nature* 448 (7151), 338–341.
- Lee, H., Rho, J., Messersmith, P.B., 2009. *Advanced Materials* 21 (4), 431–434.
- Lee, H., Scherer, N.F., Messersmith, P.B., 2006. *Proceedings of the National Academy of Sciences* 103 (35), 12999–13003.
- Lei, H.T., Shen, Y.D., Song, L.J., Yang, J.Y., Chevallier, O.P., Haughey, S.A., Wang, H., Sun, Y.M., Elliott, C.T., 2010. *Analytica Chimica Acta* 665 (1), 84–90.
- Lei, J.P., Ju, H.X., 2012. *Chemical Society Reviews* 41 (6), 2122–2134.
- Lin, M.H., Liu, Y.J., Liu, C.H., Yang, Z.H., Huang, Y.B., 2011. *Biosensors and Bioelectronics* 26 (9), 3761–3767.
- Lin, M.H., Liu, Y.J., Sun, Z.H., Zhang, S.L., Yang, Z.H., Ni, C.L., 2012a. *Analytica Chimica Acta* 722, 100–106.
- Lin, M.H., Liu, Y.J., Yang, Z.H., Huang, Y.B., Sun, Z.H., He, Y., Ni, C.L., 2012b. *International Journal of Electrochemical Science* 7 (2), 965–978.
- Liu, H.Y., Wu, X.M., Zhang, X., Burda, C., Zhu, J.J., 2012. *Journal of Physical Chemistry C* 116 (3), 2548–2554.
- Mani, V., Chikkaveeraiah, B.V., Patel, V., Gutkind, J.S., Rusling, J.F., 2009. *ACS Nano* 3 (3), 585–594.
- Munsch, C., Héas-Moisan, K., Tixier, C., Boulesteix, L., Morin, J., 2011. *Science of Total Environment* 409 (21), 4618–4627.
- Qu, L., Xia, S.H., Bian, C., Sun, J.Z., Han, J.H., 2009. *Biosensors and Bioelectronics* 24 (12), 3419–3424.
- Ricci, F., Volpe, G., Micheli, L., Palleschi, G., 2007. *Analytica Chimica Acta* 605 (2), 111–129.
- Singh, K., Rahman, M.A., Son, J.L., Kim, K.C., Shim, Y.-B., 2008. *Biosensors and Bioelectronics* 23 (11), 1595–1601.
- Sun, X.M., Li, Y.D., 2004. *Angewandte Chemie International Edition* 43 (5), 597–601.
- Tanabe, S., 2008. *Marine Pollution Bulletin* 57 (6–12), 267–274.
- Wan, Y., Wang, Y., Wu, J.J., Zhang, D., 2011a. *Analytical Chemistry* 83 (3), 648–653.
- Wan, Y., Zhang, D., Wang, Y., Qi, P., Hou, B.R., 2011b. *Biosensors and Bioelectronics* 26 (5), 2595–2600.
- Wang, G.F., Huang, H., Zhang, G., Zhang, X.J., Fang, B., Wang, L., 2011a. *Langmuir* 27 (3), 1224–1231.
- Wang, Q., Haughey, S.A., Sun, Y.M., Eremin, S.A., Li, Z.F., Liu, H., Xu, Z.L., Shen, Y.D., Lei, H.T., 2011b. *Analytical and Bioanalytical Chemistry* 399 (6), 2275–2284.
- Yang, S.Y., Zhao, C., Ge, C.Y., Dong, X.M., Liu, X.T., Liu, Y.J., Fang, Y.P., Wang, H.Q., Li, Z.S., 2012. *Journal of Materials Chemistry* 22 (15), 7104–7107.
- Yang, W.R., Ratnac, K.R., Ringer, S.P., Thordarson, P., Gooding, J.J., Braet, F., 2010. *Angewandte Chemie International Edition* 49 (12), 2114–2138.
- Yu, X., Munge, B., Patel, V., Jensen, G., Bhirde, A., Gong, J.D., Kim, S.N., Gillespie, J., Gutkind, J.S., Papadimitrakopoulos, F., Rusling, J.F., 2006. *Journal of American Chemical Society* 128 (34), 11199–11205.
- Yu, X.Y., Yang, S.Y., Zhang, B.H., Shao, D., Dong, X.M., Fang, Y.P., Li, Z.S., Wang, H.Q., 2011. *Journal of Materials Chemistry* 21 (33), 12295–12302.
- Zhang, B.H., Yu, X.Y., Ge, C.Y., Dong, X.M., Fang, Y.P., Li, Z.T., Wang, H.Q., 2010. *Chemical Communications* 46 (48), 9188–9190.
- Zheng, T.T., Zhang, R., Zou, L.F., Zhu, J.J., 2012. *Analyst* 137 (6), 1316–1318.
- Zhu, Y., Son, J.L., Shim, Y.-B., 2010. *Biosensors and Bioelectronics* 26 (3), 1002–1008.
- Zou, Y.Q., Wang, Y., 2011. *ACS Nano* 5 (10), 8108–8114.